

Calculation of Triode Constants*

By J. H. FREMLIN, M.A., Ph.D., A.Inst.P.

SUMMARY.—*A new treatment of the equivalent diode is proposed, from which formulæ for anode current and mutual conductance in plane or cylindrical triodes are obtained in terms of the penetration factor, the inter-electrode distances, and the voltages applied to grid and anode. In the plane case the values found differ from those given by the most widely used expressions by a factor*

$$\left[\frac{1 + D}{1 + D \left(\frac{l_a}{l_g} \right)^{4/3}} \right]^{3/2},$$

which may in some circumstances be considerably less than 1.

In the cylindrical case a similar but more complex factor is obtained. The expressions obtained for the plane case are shown experimentally to be more nearly correct than previous expressions.

These formulæ can only be used in cases for which the penetration factor can be calculated. Beginning with Maxwell's expression for the potential distribution due to a charged grid of fine wires it is shown how this distribution can be calculated for the case of a grid close to the cathode (Appendix D), and hence the value of penetration factor can be calculated for zero current at these close spacings.

It is shown experimentally that the value of penetration factor thus obtained may be used with some accuracy up to considerable current densities. Calculated and experimental values of mutual conductance at close spacings are compared, and it is shown that if allowance is made for emission velocity very close agreement can be obtained down to values of grid-cathode clearance of only a few per cent. of the grid pitch. A definite maximum value of mutual conductance for constant current density is shown to occur at a cathode-grid clearance of the order of half the grid pitch.

INTRODUCTION

IT is of fundamental importance in the design and in the development of thermionic valves to be able to determine in advance what the characteristics of such valves will be. In the case of a diode it is already possible to do this to a very considerable accuracy when the electrodes are either parallel planes or concentric cylinders. Where there are one or more grids between the anode and the cathode, however, the position is less satisfactory. Schottky, Miller¹, King², and others have derived expressions for the amplification factor μ of an infinite plane triode and of a cylindrical triode of infinite length in which the ratio $\frac{\text{wire diameter}}{\text{grid pitch}}$, d/a , is assumed small (less than 0.1). Vogdes and Elder³ have obtained a formula available for larger values of d/a up to about one-third, and Ollendorff⁴ gives a method of calculation said to be valid for all values of d/a . The theoretical values of

μ agree very well with experiment so long as the distance of the grid from the cathode l_g is greater than about one grid pitch.

Calculations of anode current per unit area i and mutual conductance per unit area g_m are not usually as successful, though a large number of formulæ have been proposed both on theoretical and on empirical grounds. The work described in this paper was undertaken in the attempt to make more accurate calculations possible for triodes. It was especially concerned with the case in which the grid is very close to the cathode, for which relatively little experimental work has been published. Before an expression could be developed for this case it was necessary to investigate the expressions for current in the simpler conditions where the wires of the grid are thin and where the cathode-grid distance is appreciably more than one grid pitch.

In Part I theoretical formulæ are developed for i and g_m when the cathode-grid distance is greater than the grid pitch, and the apparatus used for testing these is described.

In Part II it is shown how these formulæ may be used when the grid is very close to the

* Republished from the *Philosophical Magazine and Journal of Science*, Vol. 27, No. 185, June 1939.

¹ For numbered references see Appendix B.

cathode so long as the reduction of penetration factor is taken into account.†

Definitions of the symbols used and a table of references are given at the end in Appendices A and B.

PART I

THEORY

The expressions most frequently used⁵ for anode current and mutual conductance are (omitting a small contact-potential term):

$$i = \frac{2.34 \times 10^{-6}(V_g + DV_a)^{3/2}}{l_g^2(1 + D)^{3/2}} \dots\dots(1)$$

amps. per unit area,

where V_aV_g are the anode and grid potentials, D is the penetration factor (reciprocal of the amplification factor), and l_g is the distance of the plane of the grid from that of the cathode, and

$$g_m = \frac{\partial i}{\partial V_g} = \frac{3.51 \times 10^{-6}\sqrt{V_g + DV_a}}{l_g^2(1 + D)^{3/2}} \dots(2)$$

amps. per volt per unit area

for the plane case, and

$$i_t = \frac{1.47 \times 10^{-5}(V_g + DV_a)^{3/2}}{r_g\beta_{cg}^2(1 + D)^{3/2}} \dots\dots(3)$$

amps. per unit length,

$$g_m = \frac{2.20 \times 10^{-5}\sqrt{V_g + DV_a}}{r_g\beta_{cg}^2(1 + D)^{3/2}} \dots\dots\dots(4)$$

amps. per volt per unit length

for the cylindrical case⁵. Here r_g is the radius of the grid cylinder and β_{cg}^2 is a function of r_g/r_c (where r_c is the cathode radius) given by Langmuir⁷.

These formulæ were not calculated directly for a triode, but indirectly as follows. Child⁶ and Langmuir⁷ showed how the space-charge limited current could be calculated through any diode, the electrodes of which were infinite parallel planes or infinite concentric cylinders. Then, if it could be proved that the current through a given triode was exactly that which

would pass through a particular diode whose dimensions and anode potential were known, this current would be known. The particular diode is called the "equivalent diode." Its electrode parameters naturally depend upon those of the triode to which it is equivalent, and if the conception is to be of value they must be calculable in terms of these.

The formulæ (1) and (2) above were calculated on the simple assumption, without detailed analysis, that the diode with cathode-anode distance l_D given by

$$l_D = l_g \dots\dots\dots(5a)$$

and with anode voltage V_D given by

$$V_D = V_g + DV_a \dots\dots\dots(5b)$$

was nearly equivalent to the triode. The derivation of the correction factor $\frac{1}{(1 + D)^{3/2}}$

is given by (among others) Chaffee⁸; the reasoning seems at times to be somewhat obscure. Formulæ (3) and (4) were found similarly, assuming $r_D = r_g$. Other authors have made different but still arbitrary assumptions. For example, Miller¹ assumed that a diode giving the same cathode field as the triode in the absence of space-charge, and having its anode in the same position as the anode of the triode, would give the same current. His formula is as follows:

$$i = \frac{2.34 \times 10^{-6}(V_g + DV_a)^{3/2}}{\sqrt{l_a}(l_g + Dl_a)^{3/2}}$$

amperes per unit area.

Owing to the assumption that

$$l_D = l_a$$

this underestimates the current considerably and is not much used.

Benham¹³ has recently put forward reasons why a formula similar to Miller's, but putting l_D instead of l_a , where

$$l_D = l_g + Dl_a,$$

should be accepted. Unlike Miller's formula this ensures that the denominator tends correctly to l_g^2 as D becomes very small.

For large values of D (0.1 or above, say, for ordinary valve dimensions) these formulæ particularly Benham's, give more nearly the current which is determined experimentally than does formula (1) given above. It does not, however, seem to have been realized that

† Throughout this paper the quantity "penetration factor," sometimes described as "Durchgriff," is in general used in preference to its reciprocal, the amplification factor. The use of the term "amplification factor" seems rather inapt in many cases, particularly in the consideration of electrostatic problems, and is therefore confined to cases in which its physical meaning is clear.

it is possible to calculate the current through a triode without direct reference to a particular equivalent diode. This can be done as follows. Consider first the plane case.

If a current of density i is flowing between plane electrodes under space-charge limited conditions, the potential distribution will be given by

$$V^{3/2} = kil^2, \dots\dots\dots(6)$$

where $k = \frac{1}{2.34 \times 10^{-6}}$ if i is measured in

amps. per sq. cm and V is measured in volts. Here the cathode is taken as origin of V and of l , and the effects of initial velocity of the electrons are neglected. Equation (6) then merely expresses the Child-Langmuir law. The distribution is shown in Fig. 1. Suppose that the anode and grid of the triode are introduced into the electron stream at such potentials that the original distribution is unaltered, i.e., so that

$$\left. \begin{aligned} V_a &= k^{2/3} i^{2/3} l_a^{4/3}, \\ V_g &= k^{2/3} i^{2/3} l_g^{4/3}. \end{aligned} \right\} \dots\dots\dots(7)$$

We have now a triode with electrode potentials which are known in terms of the total space current which is passing. It is known that the field at the cathode of a plane triode is given by

$$\frac{\partial V}{\partial l} = \frac{V_g + DV_a}{l_g + Dl_a} \dots\dots\dots(8)$$

in the absence of space-charge⁹. When a space-

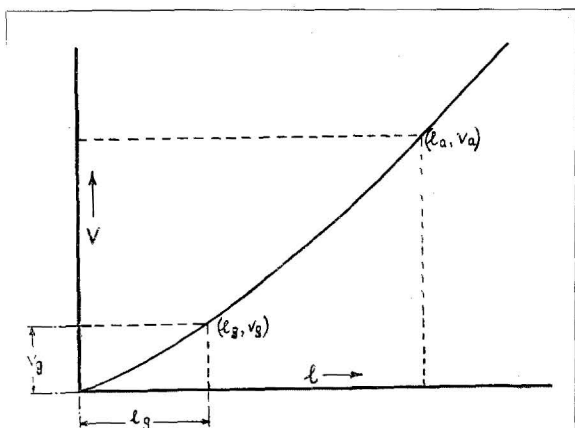


Fig. 1—The curve represents the potential distribution in a plane triode when the charge on the grid is zero and a space charge limited current i is flowing; the potential V at any distance l from the cathode is then given by $V^{3/2} = kil^2$.

charge-limited current flows, the cathode field is reduced to zero, and it is known that for any electrode system the current required to do this is proportional to the three-halves power of the cathode field. Hence we know that

$$i = K(V_g + DV_a)^{3/2}, \dots\dots\dots(9)$$

where K depends on the dimensions of the valve.

Substituting from (7) for V_g, V_a , we have

$$i = K(k^{2/3} i^{2/3} l_g^{4/3} + Dk^{2/3} i^{2/3} l_a^{4/3})^{3/2};$$

$$\therefore K = \frac{1}{k(l_g^{4/3} + D l_a^{4/3})^{3/2}};$$

$$\therefore K = \frac{2.34 \times 10^{-6}}{[l_g^{4/3} + D l_a^{4/3}]^{3/2}} \text{ in practical units. } \dots(10)$$

Hence

$$i = \frac{2.34 \times 10^{-6} (V_g + DV_a)^{3/2}}{[l_g^{4/3} + D l_a^{4/3}]^{3/2}} \dots\dots(11)$$

amps. per unit area,

whence we have

$$g_m = \frac{3.50 \times 10^{-6} \sqrt{V_g + DV_a}}{[l_g^{4/3} + D l_a^{4/3}]^{3/2}} \dots\dots(12a)$$

amps. per volt per unit area.

From (11) and (12a) we have also

$$g_m = \frac{2.64 \times 10^{-4} i^{1/3}}{[l_g^{4/3} + D l_a^{4/3}]} \dots\dots\dots(12b)$$

amps. per volt per unit area.

These differ from the usual formulæ used only in the replacement of the term $[1 + D]^{3/2}$ by the term

$$\left[1 + D \left(\frac{l_a}{l_g} \right)^{4/3} \right]^{3/2}.$$

It will be noticed that the equation for current has been derived without explicit reference to the equivalent diode. The form of the equations shows that the triode is equivalent to a particular diode, however, whose dimensions and anode potential (from equations (8) and (11)) are given by

$$l_D = \frac{[l_g^{4/3} + D l_a^{4/3}]^3}{[l_g + D l_a]^3};$$

$$V_D = \frac{[l_g^{4/3} + D l_a^{4/3}]^3}{[l_g + D l_a]^4} [V_g + DV_a]. \dots\dots(13)$$

The difference between this value of l_D and the

values hitherto assumed expresses the difference between equation (11) and previous formulæ which have been given for current. Diodes giving the same cathode fields in the absence of current, but having different electrode spacings, pass different currents, and the importance of this fact has not been sufficiently realized.

No mention has been made so far either of the fact that part of the current will be stopped by the grid wires when these are positive or of the possible variation of the penetration factor. The effect of the former will always be very small, as if the wires are relatively thin the current will be little affected, while if they are thick the space-charge between grid and anode will anyway be largely shielded from the cathode.

If the penetration factor varies very rapidly the formulæ (12a) and (12b) may be in error, owing to the existence of appreciable terms involving

$$\frac{\partial D}{\partial V_g} \quad \text{and} \quad \frac{\partial D}{\partial V_a} .$$

The non-uniformity of space-charge owing to focusing by the grid wires when the grid is negative will not affect the field of the space-charge at the cathode so long as the grid is far enough away for its own field to be uniform.

A similar analysis has been carried out to determine the radius and potential of the anode of the equivalent diode for the case of a cylindrical triode. Given that D can be calculated, the results apply equally well to the squirrel-cage or helical grid in the absence of "inselbildung."* Large grid supports, however, cause a definite "beam" effect which makes many circular section valves obey the formulæ for planes much more closely than they do those for cylinders. With these provisos then we have

$$i_i = \frac{14.7 + 10^{-6}(V_g + DV_a)^{3/2}}{D[(r_a\beta_{ca}^2)^{2/3} + (r_g\beta_{cg}^2)^{2/3}]^{3/2}} \dots(14a)$$

amps. per unit length,

$$g_m = \frac{22.0 \times 10^{-6}\sqrt{V_g + DV_a}}{[(r_g\beta_{cg}^2)^{2/3} + D(r_a\beta_{ca}^2)^{2/3}]^{3/2}} \dots(14b)$$

amps. per volt per unit length.

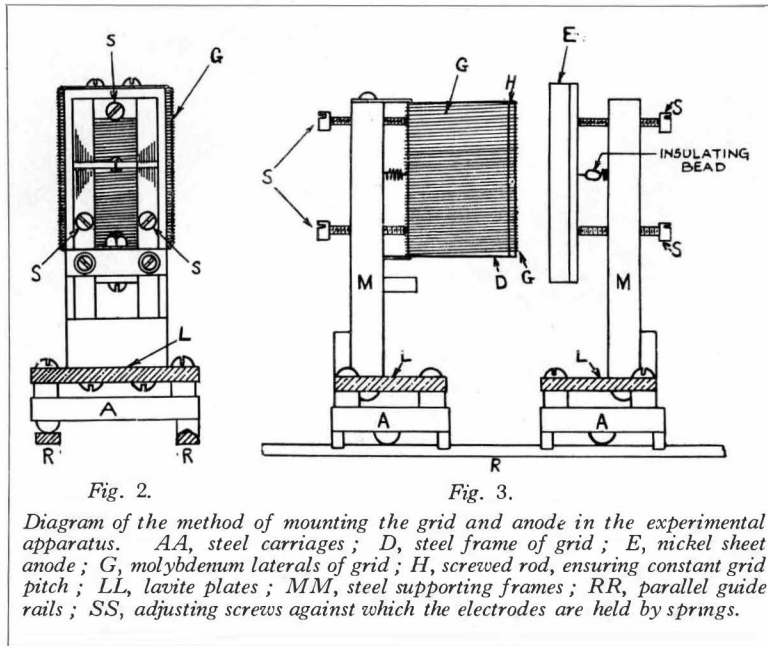
The effect of initial velocities has been neglected throughout this discussion. In the case of the plane diode Langmuir¹⁰ has calculated rigorously the potential distribution during flow of current assuming a Maxwellian distribution of emission velocity among the electrons. It would in principle be possible to calculate the equivalent diode on this basis in a manner similar to the above. It is not possible in practice, however, to obtain separate expressions for l_D and V_D , the spacing and voltage of the equivalent diode, though it can be seen that l_D would in general vary with current.

It is possible to obtain a first approximation to the true values by measuring the distances and voltages from the potential minimum rather than from the cathode itself when the distance l_m of this from the cathode can be calculated. It is not difficult to find l_m if the cathode temperature is known, for currents a small fraction of the saturation current, using the formulæ developed by Langmuir. For large currents, approaching the saturation value, initial velocity effects may be neglected. In Appendix C is estimated the correction required to allow for emission velocities to this degree of approximation.

EXPERIMENT

An apparatus has been built by means of which the grid and anode of a plane triode may be moved about at will while the current is flowing. It was desired that the position of the electrodes with respect to one another should be very accurately adjustable over a range of 2 to 3 centimetres. To do this a short but accurate optical bench was built of steel. This was fixed rigidly to a circular steel base, and covered by a bell-jar which was sealed to the base with Apiezon Q. A pumping tube, a tube leading to an ionization manometer, and a tube carrying the necessary insulated electrical leads were soldered into the base, and the whole system could be evacuated by means of an oil-diffusion pump backed by a Cenco Hivac. In Figs. 2 and 3 are shown diagrams of the carriages and frames which were used to support anode and grid. In each case to the small steel carriage A sliding upon the optical bench was bolted a sheet of steatite to which

* The term "inselbildung" is here taken to mean the state of affairs in which emission from the cathode surface is appreciably non-uniform.

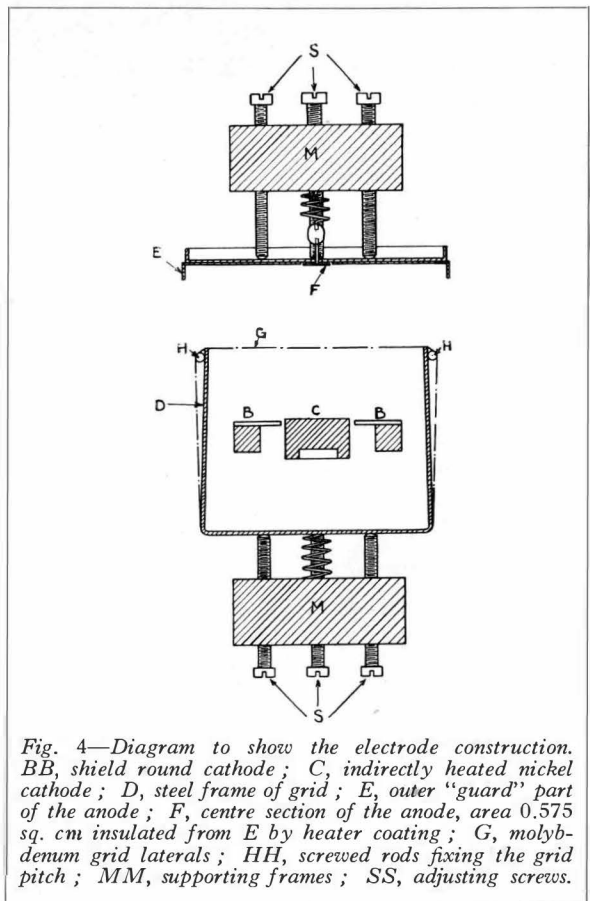


the frame M was fixed. The plane of each electrode was adjustable by means of the three screws S, against which the electrode itself was held by a molybdenum spring. The two carriages were moved by means of screwed rods (not shown) operated by steel ground joints lubricated with Apiezon L grease, and the positions of the electrodes were determined by graduations on the moving parts of the ground joints. As the screw used was of exactly 1 mm pitch, one complete rotation represented 1 mm movement of the carriage. It was possible to set the position of either electrode repeatedly to an accuracy of 0.01 mm. In Fig. 3 the cathode support is omitted for the sake of clarity; this was bolted rigidly to the steel base, perpendicular to the steel rails on which the carriages ran. An indirectly heated coated cathode C was used, mounted on steatite insulators attached to a steel supporting frame shown in section at B in Fig. 4. The cathode itself was of unconventional type, as it was necessary to ensure absolute flatness. The working part consisted of a solid piece of nickel, 30 mm by 8 mm by 5 mm thick, ground accurately flat on one face. The heater was contained in a shallow channel milled in the back, and was held in by two or three layers of thin nickel sheet, very lightly attached, to reduce radiation losses. As is indicated by the

section of the whole electrode system shown in Fig. 4, one face only of the cathode C was coated and used.

The cathode C and the frame B (from which it was insulated) were completely surrounded by the light steel frame D carrying the grid wires G. In order that the grid wires should be truly coplanar they were wound upon this frame, of which the edges were very carefully ground flat and parallel. To ensure even pitch two light screwed rods H were welded near the edges of D, and the wires of the grid were wound into the threads at suitable intervals. This avoided the small irregularities always produced by welding. The grid could be

produced by welding. The grid could be



adjusted parallel to the cathode extremely well, so that measurements could be made down to a clearing distance of 0.002 cm between the cathode coating and the inner side of the grid wires, although the working length of the grid was 3 cm.

In order to investigate the variation of current and mutual conductance in a planar triode without disturbing edge effects the anode was made of nickel sheet in guard ring form. A small rectangular section F (Fig. 4) was insulated from the main body of the anode E by a thin coating of insulating paste, the whole being baked at red heat *in vacuo* before use. This guard ring structure, though absolutely necessary, was not quite so flat as were the cathode and grid. The position of the centre section F, 1.550 cm long by 0.371 cm broad, was known to 0.004 cm, and the anode at no place departed from flatness by more than this amount.

An ionization gauge was used to measure the pressure. Between it and the apparatus was a small trap which could be surrounded by liquid air. This made it easy to distinguish between air and condensable vapour, and made the finding of leaks a practically painless process. During the experimental work the pressure was maintained at between 5×10^{-7} and 3×10^{-6} mm; the apparatus could be degassed enough for this by running for about a day after the initial activation of the cathode.

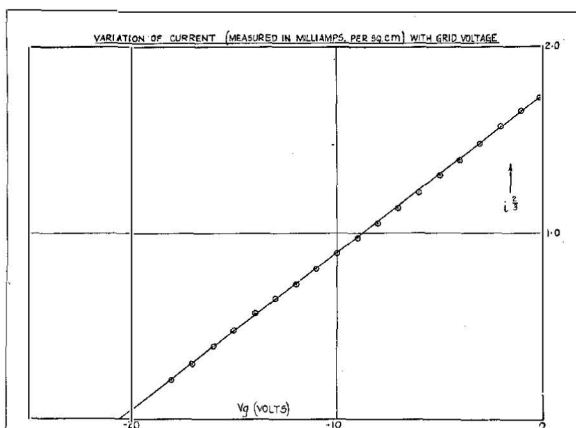


Fig. 5—This shows the variation of anode current density i with grid potential V_g , indicating that the three-halves power law is closely obeyed. Anode potential was 200 volts and the dimensions were as follows: $l_g = 0.170$ cm; $l_a = 0.773$ cm; $a = 0.175$ cm; $d = 0.0089$ cm.

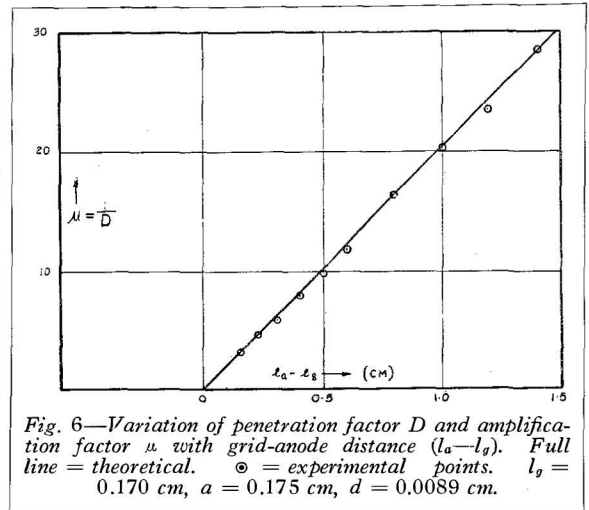


Fig. 6—Variation of penetration factor D and amplification factor μ with grid-anode distance ($l_a - l_g$). Full line = theoretical. \odot = experimental points. $l_g = 0.170$ cm, $a = 0.175$ cm, $d = 0.0089$ cm.

Tests were made to see whether the anode structure was properly carrying out its function of eliminating edge effects. If the edge effects were eliminated, changes in them must also have been eliminated. They could readily be changed by altering the potential V_B with respect to the cathode of the frame B round the cathode (Fig. 4) (B was usually maintained at cathode potential). A grid potential of zero and an anode potential of 200 volts were maintained, the grid being in position midway between anode and cathode. A change from -15 to $+15$ volts of V_B produced no detectable change in the current to the centre section of the anode, I_F , though the current to the outer part of the anode, I_E , was doubled. Change of V_B from -30 volts to $+30$ volts gave a change of I_F from 1.00 to 1.04 mA, while I_E changed from 5 mA to 15 mA.

It seems clear from this that the guard ring was effective. The value of I_F was very sensitive, however, owing to secondary emission, to any small potential difference between E and F (Fig. 4). A change of 1 volt sometimes made a difference of more than 10 per cent. in I_F . Care was taken therefore during all experimental work to ensure that no potential difference was set up; it was hoped that contact potential differences would be small, as E and F were made from the same sample of nickel and were treated similarly throughout.

Figs. 5-9 show some results of the experiments. First, tests were made of amplification factor to see whether the Miller-Schottky

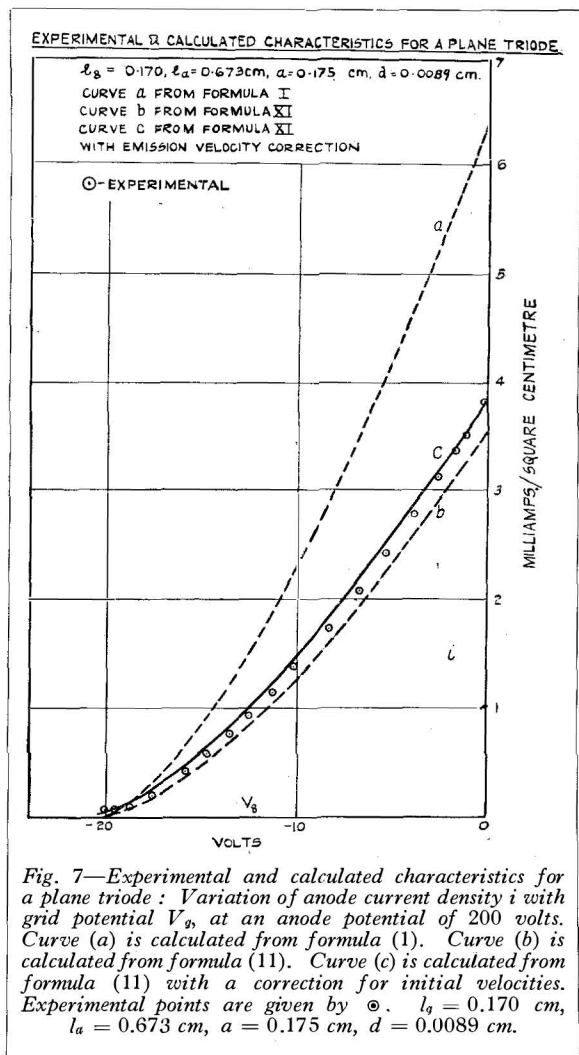


Fig. 7—Experimental and calculated characteristics for a plane triode: Variation of anode current density i with grid potential V_g , at an anode potential of 200 volts. Curve (a) is calculated from formula (1). Curve (b) is calculated from formula (11). Curve (c) is calculated from formula (11) with a correction for initial velocities. Experimental points are given by \odot . $l_g = 0.170$ cm, $l_a = 0.673$ cm, $a = 0.175$ cm, $d = 0.0089$ cm.

formula* could be trusted for the values of d/a , with which it was desired to work. Owing to the double anode construction it was difficult to measure the amplification factor dynamically, and the most accurate method was found to be extrapolation of a line obtained by plotting $I_F^{2/3}$ against V_g to zero current. This method also gave confirmation of the fact that current obeyed the three-halves-power law (see Fig. 5).

Fig. 6 shows that good agreement between

* See ref. 1. For plane electrodes this is

$$\mu = \frac{2\pi(l_a - l_g)}{1} \frac{1}{a \log_e \frac{\pi d}{2a}}$$

($l_a - l_g$) is the distance between grid and anode planes, a is the grid pitch, and d is the grid wire diameter.

calculated and observed amplification factor was obtained. This being so, the relations obtained for current and mutual conductance could fairly be tested.

In Fig. 7 are shown actual measured values of anode current together with curves calculated from equation (1) (curve a) and equation (11) (curve b). It can be seen that curve (b) is considerably more accurate than (a), but that nevertheless equation (11) appreciably underestimates the current. This is very largely accounted for if we take into account the effects of the emission velocity. Curve (c) is calculated from equation (11) as before, but replacing l_g and l_a by $l_g - l_m$ and $l_a - l$ respectively, as is shown in Appendix C, i.e., the position of the potential minimum is calculated and all distances measured therefrom instead of from the cathode surface.

The introduction of a filament for the accurate measurement of contact potential would

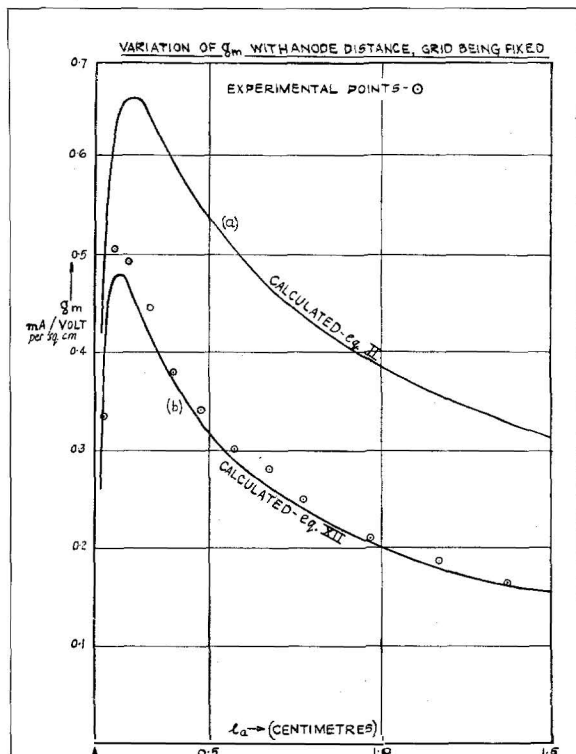
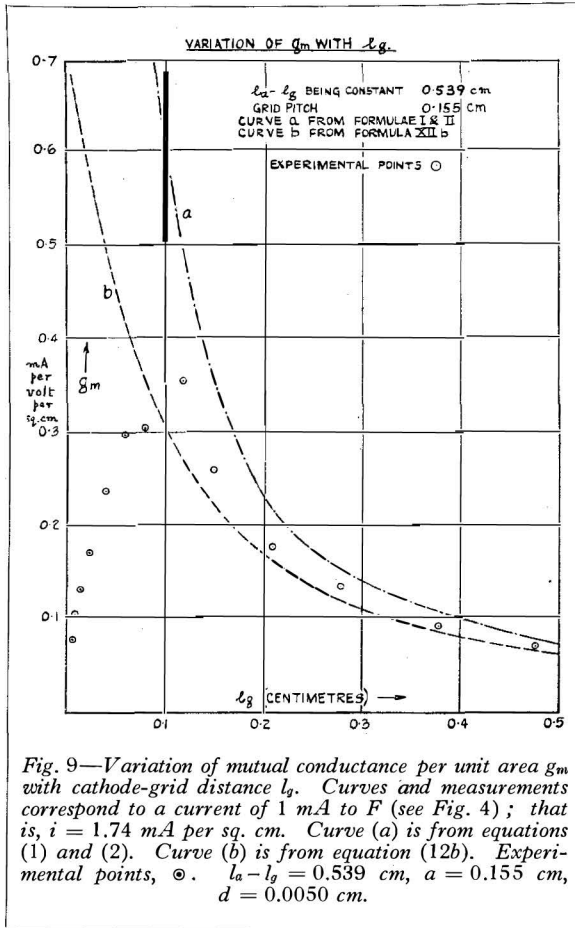


Fig. 8—Variation of mutual conductance per unit area g_m with cathode-anode distance l_a at $V_a = 200$ volts, $V_g = 0$. $l_g = 0.170$ cm, $a = 0.175$ cm, $d = 0.0089$ cm. Curve (a) is calculated from equation (2). Curve (b) is calculated from equation (12a). Experimental points are given by \odot .



If the initial velocity correction were made to equation (1) the disagreement with the experiment would be made appreciably worse instead of better, but when applied to equation (11) the agreement with experiment becomes very satisfactory. It is usually more important to be able to calculate the mutual conductance than the current so, having shown the possibility of the latter, current calculations will not be further considered in Part I.

As with amplification factor, the mutual conductance is difficult to measure dynamically, and all measurements were made on anode current-grid voltage characteristics. In Fig. 8 is shown the comparison between theory and experiment for the variation of mutual conductance measured at $V_g = 0$ with anode distance, the grid distance being kept fixed. In this experiment the correction for initial velocities, always smaller for mutual conductance than for current, has not been made. Making the correction would raise the calculated value of g_m at any given value of anode distance by something of the order of about 2 per cent.; the two curves could not easily be shown in a reproduction. Equation (12) derived from the theory proposed above, clearly gives much better agreement than does the more frequently used equation (2).

have involved considerable constructional difficulties, and was not attempted.

The effective contact potential between the grid and the cathode was found merely by measuring the applied grid potential for which grid current disappeared (using a microammeter) when a plate current of 10 mA/sq. cm was flowing, the grid being close to the cathode. This gives the applied grid potential corresponding to the potential minimum rather than to the cathode surface itself. In the particular case of Fig. 7 the value of V_m would be about -0.2 volts. All the curves shown are corrected to the true value of cathode potential calculated in this way though the effect of the correction is very small.

The current was always small compared to the saturation current available (about 80 mA/sq. cm), and in these circumstances l_m can easily be found from the relation given by Langmuir¹⁰ (see Appendix C).

Fig. 9 shows the variation of mutual conductance with cathode-grid distance, the grid-anode distance $l_a - l_g$ being kept constant. In this case the mutual conductance is calculated and measured for constant anode current, using equation (12b). Here it is possible to show the curve, allowing for the emission velocity correction. It can be seen that agreement is good for values of grid-cathode distance greater than the pitch, but that as soon as the grid gets closer to the cathode than this (i.e., by $l_g < a$) the experimentally measured values deviate more and more from the theory. It is particularly striking that the theory shows a continuous increase of g_m as $l_g/a \rightarrow 0$, while the experiment shows a well-marked maximum value at $l_g/a \approx 3/4$.

By a further investigation of the geometrical theory for small values of l_g/a it is possible to account quantitatively for the discrepancy, and to show why a maximum value of g_m is obtained. This investigation is described in Part II.

PART II.

DISTANCE BETWEEN CATHODE AND GRID SMALL COMPARED TO THE GRID PITCH

The formulæ worked out above are all derived upon the assumptions :

- (1) That the grid wires are thin ; the formulæ hold well as long as the wire diameter is less than 10 per cent. of the grid pitch.
- (2) That the grid pitch is itself smaller than the distances between the grid and the other two electrodes. When the distance between the grid and the cathode becomes equal to the grid pitch the formulæ will be in error by about 2 per cent. If the grid is far from the cathode the grid-anode distance may be considerably less than the grid pitch without causing serious discrepancies, as it is lack of uniformity of the field at the cathode that causes the major disturbances observable.

It has been mentioned above that formulæ already exist by means of which the penetration factor can be calculated when the grid wires are relatively thick^{3,4}. It is the purpose of this section to consider the case when the distance between grid and cathode is small. It will be assumed that the grid-anode distance is not small compared to the grid pitch ; the limitation of this will be discussed below.

The analysis is given in Appendix D ; we will give here only the principles on which the calculations were based, together with the results obtained.

In Maxwell's treatise on electricity and magnetism a function which gives the distribution of potential due to a plane charged grid of fine parallel wires is calculated. By adding to this a simple linear function of the distance from the grid plane it is possible to find the function corresponding to a grid between two conducting planes parallel to the grid plane so long as both conducting planes lie at a distance from the grid large compared to the pitch. If, however, the grid lies close to one or other of them, the field at the surface of the plane, and hence the charge upon it, is no longer uniform. This means that a linear term can no longer represent the effect of the planes upon the potential distribution. To solve the problem thus set up it is necessary to use the conception of electro-

static images. This shows that the potential distribution due to the grid and to the adjacent plane conductor is exactly the same as would be the appropriate part of the potential distribution between the grid and a similar grid, oppositely charged in the position of the optical image of the original grid in the conducting plane. Alternatively, if two similar but oppositely charged grids lie parallel to each other, with the wires of one exactly opposite to those of the other, there will be an accurately equipotential surface midway between them which can be identified as one plate of the plane triode to be considered. If a second conducting plane is at a considerable distance the addition to the combined potential functions of the grid and of its imaginary partner of a suitable linear term will adequately represent its contribution to the potential system.

In Appendix D is given the mathematical derivation of the potential function. From this an expression for the electric field at the cathode is calculated. Then it is easy to determine the value of the "electrostatic penetration factor" D_E , which represents the relative dependence of the field at any point of the cathode upon anode and grid voltages.

The general expression obtained for this is

$$D_E = \frac{\left\{ \frac{a}{4\pi l_a} \log_e \left[1 + \frac{\sinh^2 \frac{2\pi l_g}{a}}{\sin^2 \frac{\pi d}{2a}} \right] - \left(\frac{l_g}{l_a} \right)^2 \right\}}{\left\{ \frac{\sinh^2 \left(\frac{2\pi l_g}{a} \right)}{\cosh \left(\frac{2\pi l_g}{a} \right) - \cos \left(\frac{2\pi x}{a} \right)} - \frac{l_g}{l_a} \right\}} \dots (27)$$

where x is the distance along the cathode measured from a point in the cathode directly below a grid wire.

This is interesting in that it shows no dependence on the values of anode or grid voltage, i.e., the cathode field is still at all points a linear function of V_a and V_g . On the other hand, it is no longer constant over the cathode surface, but shows a periodic variation with x , i.e., as the point considered moves along the cathode.

EXPERIMENT

It is not possible to show the variation of

penetration factor with x experimentally in a vacuum tube, as in order to do so we should have to know the distribution of current along the cathode. On the other hand, it was felt that it was necessary to get some experimental check of the formula which is of importance in the consideration of variable μ effects in close-spaced valves. It is possible to do this quite accurately using a rubber sheet model such as was originally suggested by Mr. P. B. Moon¹¹, and has been described in some detail by J. R. Pierce and others¹². A rubber sheet is stretched in a horizontal plane so tightly that it does not sag appreciably under its own weight. Then if points on it are slightly displaced vertically by suitably applied pressure any points on the free parts of the sheet will conform to the equation

$$\frac{\partial^2 h}{\partial x^2} + \frac{\partial^2 h}{\partial y^2} = 0,$$

where h is the vertical displacement of the point and x, y are rectangular coordinates in a horizontal plane. This equation is of the same form as Laplace's equation for a potential distribution independent of the z axis under space-charge-free conditions, the displacement h taking the place of potential. We can then determine the form of the potential distribution for any system of electrodes whose geometry varies only in two dimensions by applying models of such electrodes to the stretched sheet, their displacements being proportional to the potentials normally carried by the electrodes. Clearly the slope of the free rubber sheet at any point will then be proportional to the potential gradient at the corresponding point in the electrostatic system to be investigated.

A model of a parallel plane triode was set up in this way. The "field" at the cathode was measured by means of a small piece of mirror lightly attached to the sheet very close to the edge of the cathode. This reflected a beam of light from a fixed source on to a fixed scale. It was then quite easy to measure D_E merely by raising the grid model through a measured height h_g and measuring the distance h_a through which the plate model has to be lowered in order just to bring the light spot back to its original place on the scale. This would correspond in a real valve to increasing the negative bias of the grid by a measured amount and then measuring the increase of anode potential required to maintain the cathode field at its original value.

This was repeated several times, and on plotting h_g against h_a a straight line was obtained of slope D_E . The mirror was used at several points along the cathode surface, and it was thus possible to determine the corresponding variation of D_E (the electrostatic value of penetration factor at a point on the cathode).

In Fig. 10 the full line shows the theoretical variation of D_E calculated for a particular case from equation (27) together with experimental points obtained from the rubber sheet model. The agreement may be regarded as confirmation of equation (27), though it is possible that mathematicians may rather regard it as proving the ability of the rubber sheet to deal with such problems as this. Certainly the measurements on the sheet give an extremely valuable means

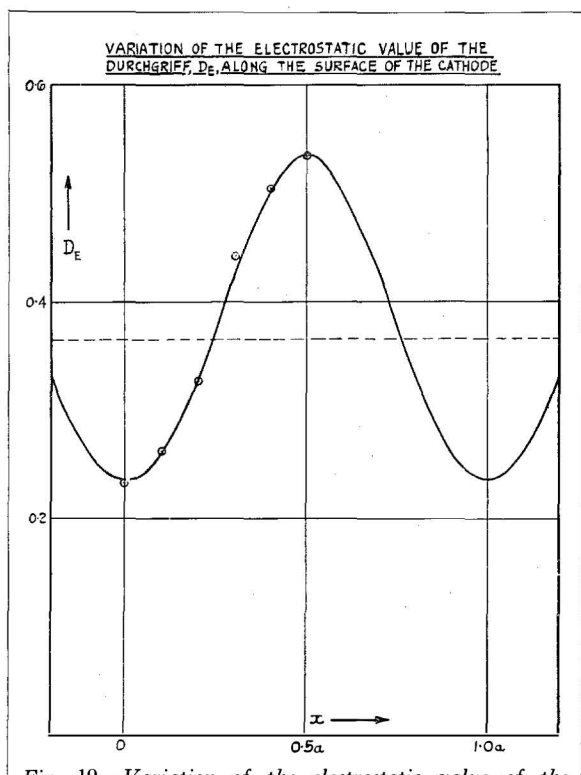
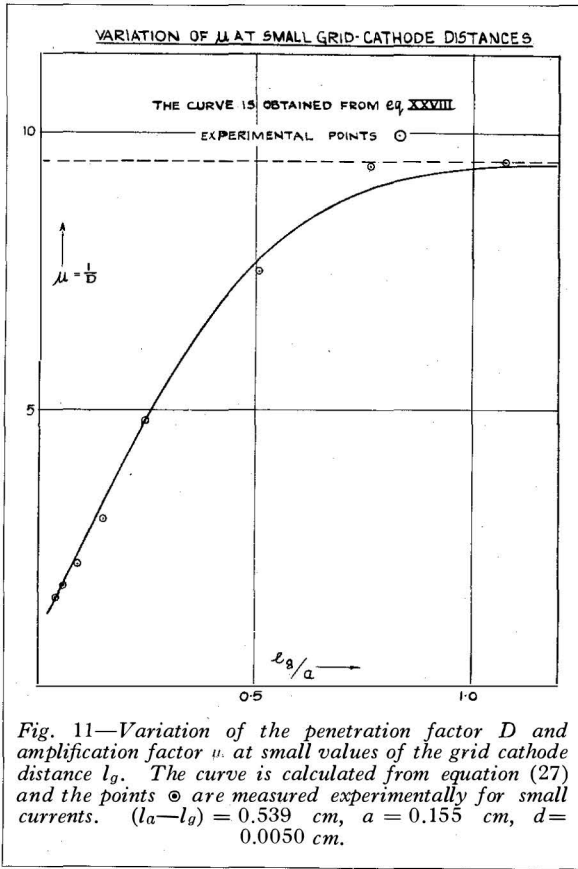


Fig. 10—Variation of the electrostatic value of the penetration factor, D_E , at a point on the cathode surface, with the distance x from a point immediately below a grid wire. The curve was calculated from equation (27) and the experimental points \odot obtained on the rubber sheet model. The dotted line shows the value of D obtained from Schottky's simple formula. $a = 29.2$ cm, $d = 0.94$ cm, $l_g = 0.4 a$, $l_a = 1.4 a$.



of measuring amplification factors in other cases which may not be as easily calculated.

Although it was not possible to measure the variation of D_E at different points of the cathode in the experimental valve, it was possible to measure the particular value D_0 of D_E when $x = (2n + 1)a/2$, this being the value which will be obtained for very small currents, as it is clear from general considerations that the current flowing very near to cut-off will be emitted by parts of the cathode midway between grid wires.

Fig. 11 shows the corresponding variation of μ_0 with l_g/a when the distance from grid to anode is kept constant; the full line was calculated from the expression

$$\mu_0 = \frac{1}{D_0} = \frac{4\pi \left[\frac{l_g}{a} - \frac{l_a}{a} \tanh \left(\frac{\pi l_g}{a} \right) \right]}{4\pi \frac{l_g}{a} \tanh \left(\frac{\pi l_g}{a} \right) - \log_e \left[1 + \frac{\sinh^2 \left(\frac{2\pi l_g}{a} \right)}{\sin^2 \left(\frac{\pi d}{2a} \right)} \right]}, \dots \dots \dots (28)$$

to which expression (27) reduces when $x = a/2$, and the experimental points were obtained by plotting μ against current and extrapolating to zero.

It seems then that the expression gives accurate values down to very small values of l_g/a . For practical reasons it has not yet been tried for very small grid-anode distances; using the rubber sheet model, agreement was still obtained for

$$\frac{l_a - l_g}{a} = 0.4 \text{ and } \frac{l_g}{a} = 0.4.$$

In order to calculate anode current and mutual conductance we need to know the variation of penetration factor with current. It can be seen from Fig. 10 that D (the average value as measured) will not begin to change very much until emission has begun over an appreciable part of the cathode surface; furthermore it will be the mean value of D_E along the emitting part of the surface weighted according to the current density; this being greatest when D_E is greatest will help to prevent a rapid change of D with small currents.

Fig. 12 shows how the experimentally measured amplification factor changed with current with the grid very close to the cathode when l_g/a was 0.039. The dotted line shows the theoretical value, $\mu_0 = 1/D_0$, for zero current. Up to a current density of 10 mA/sq. cm practically no change takes place from the cut-off value μ_0 . Beyond this μ begins to go up very rapidly as $V_g \rightarrow 0$, when current begins to flow from parts of the cathode immediately below grid wires, as would be expected. The sharpness of the "elbow" in Fig. 12 depends on the values of V_a and V_g . The type of characteristic obtained at such close spacing is shown in Fig. 13. For a given value of anode current a high anode potential and large negative grid bias will give a much sharper elbow

than will a low anode potential and correspondingly lower grid bias. The reason for this is clear at once from consideration of the way in which the current will be distributed along the cathode surface in the two cases.

For fairly small currents then it should be possible to get a close approximation to the measured mutual conductance from equation (12), using the electrostatic value for the penetration factor in the calculation, taken from equation (28). Fig. 14 shows a curve calculated in this manner for the variation of mutual conductance with l_g , assuming that 1 mA flows in the centre section of the anode used in the experiment. The calculation is carried out for the case shown in Fig. 9. The curve shows the well-marked maximum found experimentally; this is clearly demanded by the fact that when l_g/a is small g_m is proportional to $D^{-3/2}$ and D itself is roughly inversely proportional to

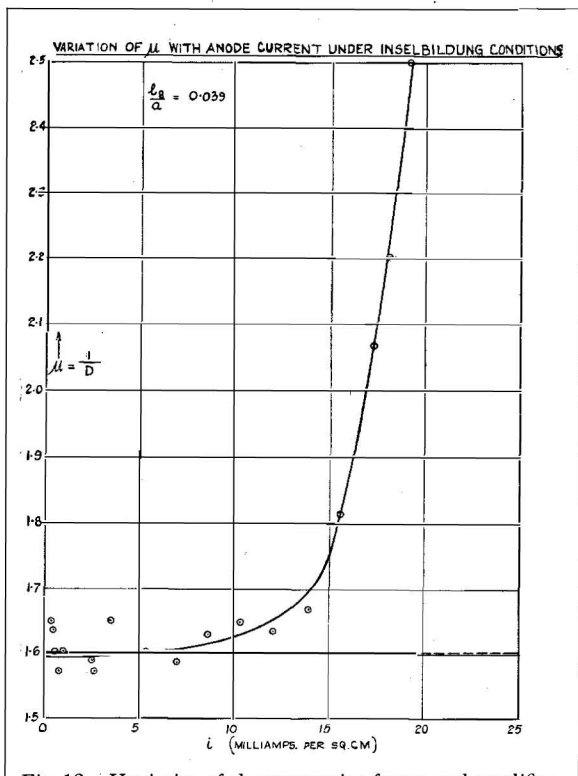


Fig. 12—Variation of the penetration factor and amplification factor with anode current density when the grid is very close to the cathode. The dotted line represents the value obtained for the cut-off value from equation (28); the points and curve are experimental. Schottky's formula gives $\mu = 1/D = 9.4$. Anode potential 140–180 volts. $l_g = 0.006$ cm, $l_a = 0.545$ cm, $a = 0.155$ cm, $d = 0.0050$ cm.

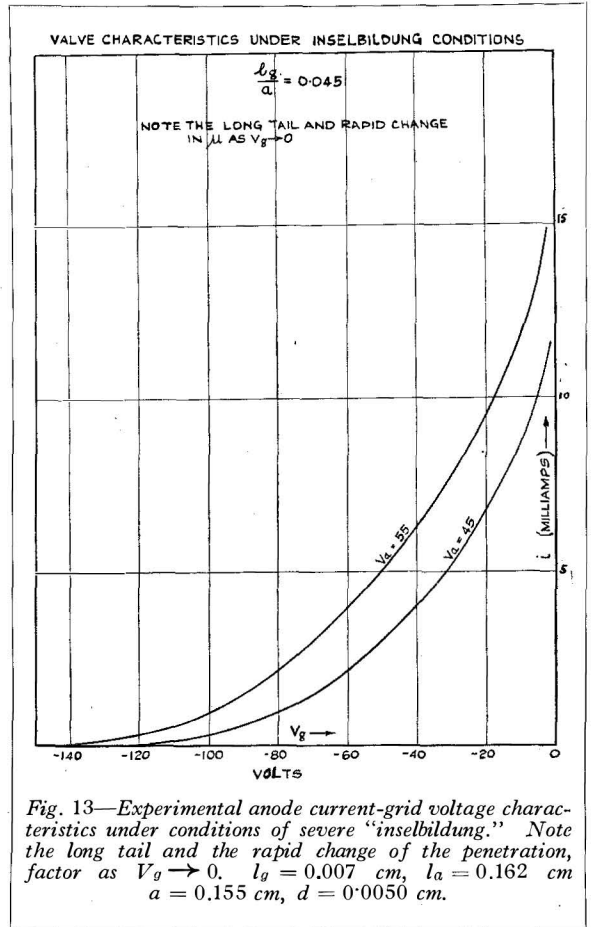


Fig. 13—Experimental anode current-grid voltage characteristics under conditions of severe "inselbildung." Note the long tail and the rapid change of the penetration factor as $V_g \rightarrow 0$. $l_g = 0.007$ cm, $l_a = 0.162$ cm, $a = 0.155$ cm, $d = 0.0050$ cm.

l_g/a^* . The values of l_g/a , for which the mutual conductance is a maximum, for constant anode-grid distance and in some other given conditions have been calculated. The calculations are not given here, as the expressions obtained are somewhat unwieldy and are of limited importance. The maxima are flat, and the exact positions found in practice depend on the emission velocities of the electrons. The experimental points shown in Fig. 9 are again put in, and it is clear that by taking account of the variation of the penetration factor with grid-cathode distance a close approximation to the measured mutual conductance can be obtained. If initial velocities are allowed for a closer approximation still can be obtained. This is clearly exemplified by Fig. 15, which was taken for a smaller value of grid-anode distance in

* This can be seen from equations (12 b) and (27); the way in which the penetration factor varies with cathode-grid distance can be seen from Fig. 11.

which the effect of emission velocity was greater and, since the saturation current was higher, more easily estimable.

We may conclude then that if allowance is made for the increase of the penetration factor at close spacings, the formulæ (11), (12) which have been developed make it possible to calculate anode current or mutual conductance to a very fair accuracy for any valve in which the electrodes may be regarded as plane, so long as the current density is not too high. Accurate calculations of the upper parts of the characteristics for close spacings have not yet been made; work is still being done on this problem. It should be noted that for valves with large amplification factors the calculated value of anode current and mutual conductance will be approximate, owing to the big difference made to the effective voltage by contact potentials, etc., unless this can be measured by observation of the grid potential at which grid current disappears. This is impossible when

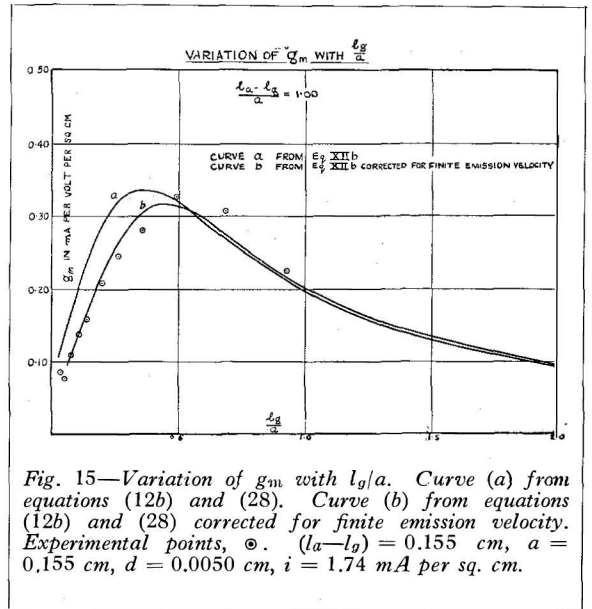


Fig. 15—Variation of g_m with l_g/a . Curve (a) from equations (12b) and (28). Curve (b) from equations (12b) and (28) corrected for finite emission velocity. Experimental points, \odot . ($l_a - l_g$) = 0.155 cm, a = 0.155 cm, d = 0.0050 cm, i = 1.74 mA per sq. cm.

it is desired to carry out the calculations in advance. It is often useful, then, to decide in advance the anode current to be used at the working point and to use the formula (12 b) :

$$g_m = \frac{26.4 \sqrt[3]{i} \times 10^{-3} \text{ amps. per volt per sq. cm}}{l_g^{4/3} + D l_a^{4/3}} \text{ when } i \text{ is in amps. per sq. cm,}$$

derived from (11) and (12 a) by elimination of V_a and V_g to determine the mutual conductance. The exact grid bias necessary is then found after the valve has been made up.

The work here described has been carried out in the Valve Laboratory of Standard Telephones and Cables, Limited, Woolwich, to whom I am indebted for permission to publish these results. I wish to acknowledge also my grateful thanks to Mr. W. T. Gibson, the Chief Valve Engineer, for the long hours which he spent in giving invaluable suggestions as to the best way of representing the results obtained; to Dr. D. H. Black, Chief of the Valve Laboratory, for his continuous advice and encouragement; to R. N. Hall and D. P. R. Petrie for their help with the work itself; and to W. R. Hindle for his skilful and accurate work in the construction of the experimental apparatus.

Finally, I would like to thank Mr. J. A. Ratcliffe for a very helpful discussion, as a result of which the theory of Part I was considerably clarified.

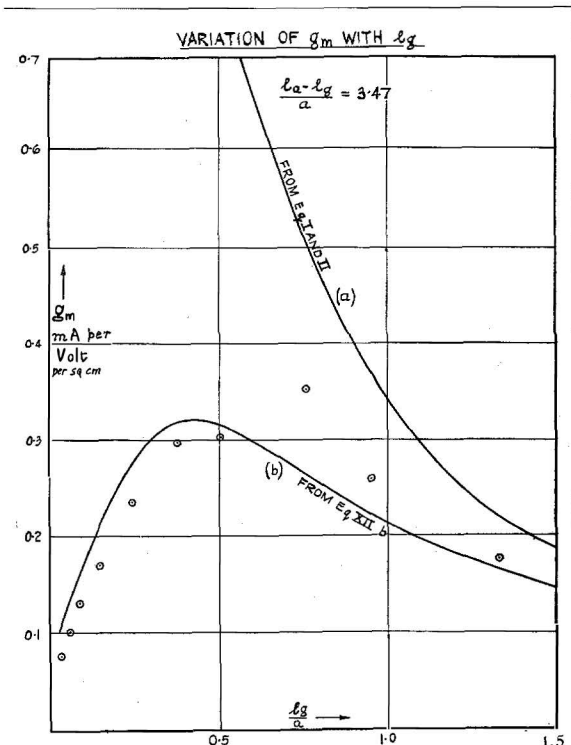


Fig. 14—Variation of mutual conductance g_m per unit area with cathode grid distance measured as a fraction of the grid pitch, l_g/a . Theoretical curves, experimental points at a current density i = 1.74 mA per sq. cm ($l_a - l_g$) = 0.539 cm, a = 0.155 cm, d = 0.0050 cm.

APPENDIX A

<i>Symbol.</i>	<i>Meaning.</i>
<i>a.</i>	Grid pitch.
<i>A, α, B.</i>	Used as constants.
$\beta^2.$	Langmuir's function for a cylindrical diode. See ref. 7.
<i>d.</i>	Diameter of a grid wire.
$D = \frac{\partial i}{\partial V_a} / \frac{\partial i}{\partial V_g}.$	Penetration factor (reciprocal of amplification factor).
$D_E = \frac{\partial}{\partial V_a} \left(\frac{\partial V}{\partial y} \right)_c / \frac{\partial}{\partial V_g} \left(\frac{\partial V}{\partial y} \right)_c.$	Penetration factor, electrostatically calculated.
$D_0.$	The value of D_E midway between wires.
<i>e.</i>	Electronic charge.
$\epsilon.$	Base of natural logarithms.
$\eta.$	The function $\frac{e}{kT}(V - V_m).$
$\eta_c.$	The value of η at the cathode; its value is $\log_\epsilon \left(\frac{i_{sat}}{i} \right).$ See ref. 10.
$g_m.$	Mutual conductance per unit area in formulæ for plane electrodes; per unit length for cylindrical electrodes.
<i>i</i> or $i_i.$	Space current per unit area (plane) or unit length (cylindrical).
$i_{sat}.$	Space current density in saturation conditions.
$I_F, I_E.$	Experimentally measured currents to the centre anode and outer guard ring respectively. See Fig. 4.
<i>k.</i>	Boltzmann's Constant.
$\xi.$	The function $4(l - l_m) \left(\frac{\pi}{2kT} \right)^{3/4} m^{1/4} (ei)^{1/2} = 2L(l - l_m).$
$\xi_c.$	The value of ξ at the cathode. See ref. 10.
<i>l.</i>	Distance of a point from the cathode.
$l_a, l_g, l_m.$	Distance of anode, grid, and potential minimum respectively from the cathode.
$l_D.$	Distance between the electrodes of the equivalent diode.
<i>L.</i>	Defined by $L = 2 \left(\frac{\pi}{kT} \right)^{3/4} m^{1/4} \sqrt{ei}.$
$\lambda.$	Charge per unit length of grid wires.
<i>m.</i>	Electronic mass.
$\mu = \frac{\partial i}{\partial V_g} / \frac{\partial i}{\partial V_a}.$	Amplification factor.
$\mu_0.$	Reciprocal of $D_0.$ (Amplification factor at cut-off).
<i>n.</i>	An integer.
$r_a, r_g, r_c.$	Radii of anode, grid, and cathode respectively of a cylindrical triode.
<i>T.</i>	Absolute temperature.
<i>V.</i>	Potential at any point.
$V_a, V_g, V_m.$	Potentials of anode, grid, and potential minimum with respect to the cathode.
<i>x, y.</i>	Rectangular coordinates with origin in the cathode, the axis of <i>x</i> being in the plane of the cathode perpendicular to the wires and the axis of <i>y</i> passing through the centre of a wire and increasing towards the anode.
$\left(\frac{\partial V}{\partial y} \right).$	The potential gradient at the cathode surface.

APPENDIX B

REFERENCES

1. J. M. Miller, *P.I.R.E.*, viii, p. 64 (1920).
2. R. W. King, *Phys. Rev.*, xv, p. 256 (1920).
3. F. B. Vogdes and F. R. Elder, *Phys. Rev.*, xxiv, p. 683 (1924).
4. F. Ollendorff, *Elektrotechnik und Maschinenbau*, lii, p. 585 (1934).
5. See, for example, Benjamin, Cosgrove, and Warren, *I.E.E.* (April 1937).
6. Child, *Phys. Rev.*, xxxii, p. 142 (1911).
7. Langmuir, *Phys. Rev.*, ii, p. 450 (1913).
8. Chaffee, *The Theory of Thermionic Vacuum Tubes*, pp. 146-7, 1st edition.
9. Dow, *Fundamentals of Engineering Electronics*, equations (82) and (111).
10. Langmuir, *Phys. Rev.*, xxi, p. 419 (1923).
11. P. B. Moon and M. L. Oliphant, *Proc. Camb. Phil. Soc.*, xxv, p. 461 (1929).
12. J. R. Pierce, *Bell Labs. Record*, xvi, p. 305 (1938); P. H. J. A. Kleynen, *Philips Techn. Rev.*, ii, p. 338 (1937).
13. W. E. Benham, *P.I.R.E.*, xxvi, p. 1093 (1938).

APPENDIX C

As a first approximation we may correct for the effect of initial velocity of emission from the cathode by measuring all distances and voltages from the potential minimum outside the cathode rather than from the cathode itself. Langmuir¹⁰ has shown that this potential minimum always exists if the current is unsaturated, and has shown how in a plane diode its distance from the cathode l_m and depth V_m can be calculated for any given current density if the saturation current density i_{sat} is known. He assumes the emitted electrons to have a Maxwellian distribution of velocities corresponding to the temperature of the cathode. For convenience he introduces the non-dimensional variables

$$\left. \begin{aligned} \eta &= \frac{e}{kT}(V - V_m), \\ \xi &= 4\left(\frac{\pi}{2kT}\right)^{3/4} m^{1/4} \cdot \sqrt{ei}(l - l_m) = 2L(l - l_m). \end{aligned} \right\} \quad (15)$$

The relation between η and ξ is then independent of the properties of any particular diode, and tables are given in the paper previously referred to from which either can be found if the other is known. Using suffices to indicate the points considered, we have $\eta_m = 0$, and Langmuir shows that

$$\eta_c = \log_{\epsilon} \frac{i_{sat}}{i}$$

Then
$$V_m = -\frac{kT}{e} \log_{\epsilon} \frac{i_{sat}}{i}$$

or in practical units

$$V_m = -\frac{T}{11\ 600} \log_{\epsilon} \frac{i_{sat}}{i} \dots \dots \dots (16)$$

To calculate the value of l_m we use the tables mentioned above to find $-\xi_c$, since η_c can be found when i_{sat} is known.

Then
$$-\xi_c = 2Ll_m,$$

and in practical units

$$l_m = \frac{-\xi_c}{2.90 \times 10^4 T^{-3/4} \sqrt{i}} = \frac{\alpha}{\sqrt{i}} \text{ say } \dots \dots (17)$$

If voltages and distances are measured from the potential minimum then, from (11), in the plane case,

$$i = \frac{2.34 \times 10^{-6} (V_g + DV_a - V_m)^{3/2}}{[(l_g - l_m)^{4/3} + D(l_a - l_m)^{4/3}]^{3/2}} \dots \dots (18)$$

amps. per unit area.

This expression, in spite of its approximate nature, would give a very complex formula for the mutual conductance as it stands, since l_m and V_m both vary with i . If i is not a large fraction of i_{sat} however, we can make some further assumptions before differentiating. For large values of η the rate of variation of $-\xi$ with η is small. If this is neglected we have, as in (17), that l_m is inversely proportional to \sqrt{i} , α being assumed constant for the purpose of differentiation. When i/i_{sat} becomes fairly large, α is no longer even approximately constant, but, on the other hand, the whole correction required is very small. The effect of the variation of V_m is very small except at very small currents indeed.

Then we have, from equation (18),

$$V_g + DV_a - V_m = 5690 \cdot i^{2/3} \left[\left(l_g - \frac{\alpha}{\sqrt{i}} \right)^{4/3} + D \left(l_a - \frac{\alpha}{\sqrt{i}} \right)^{4/3} \right];$$

$$\begin{aligned} \therefore \frac{\partial V_g}{\partial i} &= \frac{2}{3} \cdot 5690 \cdot i^{-1/3} \left[\left(l_g - \frac{\alpha}{\sqrt{i}} \right)^{4/3} + D \left(l_a - \frac{\alpha}{\sqrt{i}} \right)^{4/3} \right] \\ &+ 5690 i^{2/3} \left[\frac{2\alpha}{3} \left(l_g - \frac{\alpha}{\sqrt{i}} \right)^{1/3} i^{-3/2} + \frac{2}{3} D \alpha \left(l_a - \frac{\alpha}{\sqrt{i}} \right)^{1/3} i^{-3/2} \right], \end{aligned}$$

which gives us finally

$$g_m = g_{m1} \left[1 + l_m \frac{(l_g - l_m)^{1/3} + D(l_a - l_m)^{1/3}}{(l_g - l_m)^{4/3} + D(l_a - l_m)^{4/3}} \right]^{-1} \quad (19)$$

where g_{m1} is the value of g_m obtained from equation (12b) by replacing l_g, l_a by $(l_g - l_m), (l_a - l_m)$ respectively for a given current. The factor in the bracket is usually very close to 1.

In the case of a valve in which the electrodes are concentric cylinders the correction for initial velocities is considerably smaller¹⁰, and may therefore be neglected.

APPENDIX D

If we have a grid at a distance l_g from a conducting plane cathode we can consider the potential distribution as being that due to a pair of oppositely charged grids at $y = \pm l_g$. ($y = 0$ at the cathode). The expression

$$V = -\lambda \log_e 2 \left[\cosh \left(\frac{2\pi y}{a} \right) - \cos \left(\frac{2\pi x}{a} \right) \right]$$

represents the potential at any point (x, y) due to a plane grid of fine equidistant parallel wires with charge per unit length λ , in the plane $y = 0$, the axis of x being taken perpendicular to the grid wires and the origin being at the centre of a wire.

Then for two grids at $y = \pm l_g$ we should have

$$V = -\lambda \log_e \left[\frac{\cosh \frac{2\pi}{a} \cdot y - l_g - \cos \frac{2\pi x}{a}}{\cosh \frac{2\pi}{a} \cdot y + l_g - \cos \frac{2\pi x}{a}} \right] \dots (20)$$

If we have an anode parallel to these at a considerable distance at $y = l_a$ we shall obtain the correct potential at any point by adding $By + C$ to the potential V , where B and C are constants. At the cathode, where $y = 0$, the potential then reduces to

$$V_1 = C. \dots (21)$$

At the grid $y = l_g, x = d/2$ (the wire radius), and we have

$$V_2 = -\lambda \log_e \left[\frac{1 - \cos \left(\frac{\pi d}{a} \right)}{\cosh \left(\frac{4\pi l_g}{a} \right) - \cos \left(\frac{\pi d}{a} \right)} \right] + Bl_g + C;$$

$$\therefore V_2 = \lambda \log_e \left[1 + \frac{\sinh^2 \left(\frac{2\pi l_g}{a} \right)}{\sin^2 \left(\frac{\pi d}{2a} \right)} \right] + Bl_g + C, \dots (22)$$

and at the anode

$$V_3 = \lambda \log_e \left[\frac{\cosh \left(\frac{2\pi}{a} \cdot l_a + l_g \right)}{\cosh \left(\frac{2\pi}{a} \cdot l_a - l_g \right)} \right] + Bl_a + C$$

$$= \lambda \cdot \frac{4\pi}{a} l_g + Bl_a + C \dots (23)$$

if l_a/a is fairly large.

From the last four equations then we have

$$\left. \begin{aligned} V_g &= \lambda \log_e \left[1 + \frac{\sinh^2 \left(\frac{2\pi l_g}{a} \right)}{\sin^2 \left(\frac{\pi d}{2a} \right)} \right] + Bl_g, (a) \\ V_a &= \frac{4\pi l_g}{a} \cdot \lambda + Bl_a, (b) \\ V &= \lambda \log_e \left[\frac{\cosh \left(\frac{2\pi}{a} \cdot y + l_g \right) - \cos \left(\frac{2\pi x}{a} \right)}{\cosh \left(\frac{2\pi}{a} \cdot y - l_g \right) - \cos \left(\frac{2\pi x}{a} \right)} \right] + By, (c) \end{aligned} \right\} (24)$$

where V is now measured from the cathode.

From these we can find the potential at any point by elimination of B and λ in terms of V_a and V_g . Here, however, the field at the

cathode, $\left(\frac{\partial V}{\partial y} \right)_c$, is required. This is given,

from (24 c), by

$$\left(\frac{\partial V}{\partial y} \right)_c = \frac{\frac{4\pi}{a} \lambda \cdot \sinh \left(\frac{2\pi}{a} l_g \right)}{\cosh \left(\frac{2\pi}{a} l_g \right) - \cos \left(\frac{2\pi x}{a} \right)} + B \dots (25)$$

Eliminating λ and B from (25), (24 a), and (24 b),

$$\left(\frac{\partial V}{\partial y} \right)_c = \frac{V_a}{l_a} + \frac{(l_g V_a - l_a V_g) \frac{4\pi}{a}}{\frac{4\pi}{a} l_g^2 - l_a \log_e \left[1 + \frac{\sinh^2 \left(\frac{2\pi}{a} l_g \right)}{\sin^2 \left(\frac{\pi d}{2a} \right)} \right]}$$

$$\times \left[\frac{l_g}{l_a} + \frac{\sinh\left(\frac{2\pi}{a}l_g\right)}{\cosh\left(\frac{2\pi}{a}l_g\right) - \cos\left(\frac{2\pi x}{a}\right)} \right] \dots (26)$$

This will vary with x until

$$\cosh\left(\frac{2\pi}{a}l_g\right) \gg 1.$$

When $l_g/a = 1$ the variation will not be very great, as $\cosh 2\pi$ is about 275, but for smaller values the variation may become considerable unless $(l_gV_a - l_aV_g)$ is small.

The relative effectiveness of the grid and anode voltages then varies along the cathode. We shall define as "electrostatic penetration factor," D_E , at any point the ratio

$$\frac{\partial}{\partial V_a} \left(\frac{\partial V}{\partial y} \right)_c / \frac{\partial}{\partial V_g} \left(\frac{\partial V}{\partial y} \right)_c.$$

The value of D_E can then be found from (26) to be given by

$$\frac{\left\{ \frac{a}{4\pi l_a} \log_e \left[1 + \frac{\sinh^2\left(\frac{2\pi l_g}{a}\right)}{\sin^2\left(\frac{\pi d}{2a}\right)} \right] - \frac{l_g^2}{l_a^2} \right\}}{\left\{ \frac{\sinh\left(\frac{2\pi l_g}{a}\right)}{\cosh\left(\frac{2\pi l_g}{a}\right) - \cos\left(\frac{2\pi x}{a}\right)} - \frac{l_g}{l_a} \right\}} \dots (27)$$

which again clearly varies along the cathode surface, giving a maximum value between two wires. In Fig. 10 is shown the form of variation

for the particular case

$$\frac{l_g}{a} = 0.4, \quad \frac{l_a}{a} = 1.4.$$

The maximum value D_0 is given by

$$D_0 = \frac{1}{4\pi} \frac{\frac{4\pi}{a} l_g \tanh\left(\frac{\pi l_g}{a}\right) - \log_e \left[1 + \frac{\sinh^2\left(\frac{2\pi l_g}{a}\right)}{\sin^2\left(\frac{\pi d}{2a}\right)} \right]}{\frac{l_g}{a} - \frac{l_a}{a} \tanh\left(\frac{\pi l_g}{a}\right)} \dots (28)$$

which for small values of l_g/a reduces to

$$D_0 = \frac{\log_e \left(1 + \frac{l_g^2}{a^2} \right)}{\frac{2\pi}{a} l_g \left(\frac{\pi l_a}{a} - 1 \right)} \dots (29)$$

The theoretical and experimental variation of D_0 with l_g/a for values of the latter less than unity is shown in Fig. 11 for a constant $\frac{l_a - l_g}{a}$

$= 1$ and $\frac{d}{a} = 0.032$. As d/a increases D_0 falls away more rapidly when l_g/a decreases, and hence when a grid close to the cathode is to be used it is advantageous to use the finest possible wire to avoid as far as possible the effects of variation with current of D .

*The Valve Laboratory,
Standard Telephones and Cables, Ltd.,
North Woolwich, E.16.*